FACETS
a multidisciplinary open access science journal

RESEARCH ARTICLE

# Extreme rainfall drives early onset cyanobacterial bloom

**Megan L. Larsen[a*], Helen M. Baulch[b], Sherry L. Schiff[c], Dana F. Simon[d], Sébastien Sauvé[d], and Jason J. Venkiteswaran[a]**

[a]Department of Geography and Environmental Studies, Wilfrid Laurier University, Waterloo, ON N2L 3C5, Canada; [b]School of Environment and Sustainability, Global Institute for Water Security, University of Saskatchewan, Saskatoon, SK S7N 5C8, Canada; [c]Department of Earth and Environmental Sciences, University of Waterloo, Waterloo, ON N2L 3G1, Canada; [d]Department of Chemistry, Université de Montréal, Montréal, QC H2V 0B3, Canada

*meg.larsen87@gmail.com



## Abstract

The increasing prevalence of cyanobacteria-dominated harmful algal blooms is strongly associated with nutrient loading and changing climatic patterns. Changes to precipitation frequency and intensity, as predicted by current climate models, are likely to affect bloom development and composition through changes in nutrient fluxes and water column mixing. However, few studies have directly documented the effects of extreme precipitation events on cyanobacterial composition, biomass, and toxin production. We tracked changes in a eutrophic reservoir following an extreme precipitation event, describing an atypically early toxin-producing cyanobacterial bloom and successional progression of the phytoplankton community, toxins, and geochemistry. An increase in bioavailable phosphorus by more than 27-fold in surface waters preceded notable increases in *Aphanizomenon flos-aquae* throughout the reservoir approximately 2 weeks postevent and ~5 weeks before blooms typically occur. Anabaenopeptin-A and three microcystin congeners (microcystin-LR, -YR, and -RR) were detected at varying levels across sites during the bloom period, which lasted between 3 and 5 weeks. These findings suggest extreme rainfall can trigger early cyanobacterial bloom initiation, effectively elongating the bloom season period of potential toxicity. However, effects will vary depending on factors including the timing of rainfall and reservoir physical structure.

**Key words:** cyanobacterial bloom, extreme rainfall, phosphorus, reservoir, cyanotoxins



Citation: Larsen ML, Baulch HM, Schiff SL, Simon DF, Sauvé S, and Venkiteswaran JJ. 2020. Extreme rainfall drives early onset cyanobacterial bloom. FACETS 5: 899–920. doi:10.1139/facets-2020-0022

Handling Editor: Neil Cameron Swart

Received: March 26, 2020

Accepted: July 20, 2020

Published: November 19, 2020



Published by: Canadian Science Publishing

## Introduction

Harmful algal blooms (HABs) have increased in intensity, frequency, and distribution across Canada and the world (Orihel et al. 2012; Pick 2016; Ho et al. 2019). In Ontario alone, the number of reported HAB events between 1994 and 2009 increased by 22-fold and, by 2009, nearly half of those reported were dominated by cyanobacteria (Winter et al. 2011). This increase in cyanobacterial growth and dominance has been strongly attributed to increased nitrogen (N) and phosphorus (P) availability (Paerl and Huisman 2009; O'Neil et al. 2012; Sukenik et al. 2015; Paerl et al. 2016) and, more recently, climatic shifts. For example, thermal regime changes have resulted in earlier and warmer water temperatures (O'Reilly et al. 2015; Richardson et al. 2017), increasing the competitive advantage of certain bloom-forming cyanobacteria over other organisms (Jöhnk et al. 2008; Paerl and Huisman 2009). Despite predicted climatic changes in both temperature and precipitation patterns (IPCC 2007; McDermid et al. 2015), less attention has been given to the importance of precipitation regime

changes, which may have an even greater impact on cyanobacteria bloom dynamics due to mixing and nutrient cycles (reviewed in Reichwaldt and Ghadouani 2012).

Extreme rainfall events, both in terms of frequency and intensity, are one of the many climatic components that have changed and are predicted to continue changing over the next quarter century (Seneviratne et al. 2012; Wuebbles et al. 2014; Soulis et al. 2016; Easterling et al. 2017; Kossin et al. 2017; Bush and Lemmen 2019; Paerl et al. 2019). Depending on soil conditions, high-intensity precipitation across a watershed may mobilize large quantities of sediment as well as soil-bound and soluble nutrients resulting in notable increases to in-lake nutrient bioavailability and suspended solids (Bouvy et al. 2003; Wood et al. 2017). Increased stream flow leads to increased water column mixing, altered flushing rates and residence times, and weakened vertical stratification (Bouvy et al. 2003; Reichwaldt and Ghadouani 2012)—all factors known to influence cyanobacteria bloom development (Jacobsen and Simonsen 1993; Mitrovic et al. 2003; Paerl et al. 2016; Wood et al. 2017). However, the degree to which those factors will affect primary production in a reservoir is directly related to event timing (e.g., early vs. late summer) and the zonal gradient created by basin morphometry differences (Kimmel and Groeger 1984).

Reservoirs vary in physical, chemical, and biological properties along a spatial gradient as a result of their design and geographic placement. Impoundment systems, constructed along river reaches, are often narrow and channelized where a river enters the reservoir (riverine zone). This shallow, well-mixed zone transitions in width and depth (transitional zone) to a broader and deeper, lake-like system (lacustrine zone) (Thornton et al. 1996). Primary production and phytoplankton phenology along the riverine–transitional–lacustrine gradient is primarily mediated by light and nutrient availability, among other interacting factors (Kimmel and Groeger 1984). However, large precipitation events could potentially disrupt characteristic primary production patterns in these zones, especially if the event introduces sizable nutrient loads, increases flushing rates, or affects other water-column properties prior to or during a bloom period. For example, Wood et al. (2017) reported decreased cyanobacterial biomass following an extreme rainfall event that led to water column cooling and destratification in a shallow, eutrophic New Zealand lake. Varying responses to extreme rainfall should be anticipated given the importance of site and event-specific factors.

Changes to seasonal phytoplankton phenology, especially in terms of cyanobacterial bloom dynamics and biomass, are a great concern to water managers. Several bloom-forming cyanobacterial species such as *Aphanizomenon flos-aquae*, *Microcystis aeriginosa*, and *Anabaena (Dolichospermum) flos-aquae* synthesize an array of bioactive compounds that pose acute, chronic, and even potentially fatal health risks to humans and other organisms through dermal contact, inhalation, and (or) ingestion of contaminated waters (Chorus and Bartram 1999; Chorus et al. 2000; Codd 2000). Metabolite production as well as the composition of toxins released are complex and tied not only to the cyanobacterial species, successional patterns, and biomass, but also to various environmental parameters including N, P, temperature, light, pH, salinity, and micronutrients (Chorus and Bartram 1999), which may all be altered by intense rainfall events (Reichwaldt and Ghadouani 2012). To date, only limited information exists regarding how toxicity may change as a result of precipitation events.

Here, we document the effects of an extreme early summer rainfall event on cyanobacterial biomass and toxin dynamics in a eutrophic reservoir and contrast these effects to a second, smaller mid-summer rainfall event. Conestogo Lake (Ontario, Canada; **Fig. 1**), has experienced recurring, late-summer cyanobacterial blooms dominated by *A. flos-aquae* since 2004 (Guildford 2006; S. Cooke, personal communication 2018). On 23 June 2017, the upper Conestogo watershed experienced a record rainfall event (daily total 78 mm measured at Conestogo Dam (Grand River

Conservation Authority (GRCA) 2017, 2018)) that resulted in severe flooding and replaced ~80% of the water in Conestogo Lake during this 4.96-d event (GRCA 2018). We first evaluate how this extreme event affected the reservoir by characterizing the physical and chemical changes across reservoir spatial zones. We then follow the trajectory of bloom development and toxicity through the season to better understand how hydrological events can alter bloom occurrence and potential health risks.

# Materials and methods

## Study site

Conestogo Lake is a bottom-draw reservoir (7.35 $km^2$) located in southwestern Ontario, Canada. Built in 1958 and currently operated by the Grand River Conservation Authority (GRCA) (Mapleton Township, Ontario), the reservoir serves as a flood control and downstream river flow augmentation system. It also provides ancillary recreational benefits for fishing, boating, and ~400 summer cottages. Conestogo Lake typically fills to capacity in the spring (15 February–30 May) with water from the upper Conestogo River basin (566 $km^2$), a predominately agricultural catchment (>80%, **Fig. 1**, left). Retained waters are used during the summer and fall (June to September) to provide consistent downstream flow to the Conestogo River and Grand River. As a result of the reservoir drawdown, mean lake depth at the deepest point drops from ~18 to 11 m and residence time varies from 26 to 119 d throughout the season (GRCA 2018).

Conestogo lake is influenced both by agricultural nutrient sources and wastewater. Wastewater from upstream municipalities is discharged <1 km north of Conestogo Lake from October through the end of April every year and held in lagoons or storage ponds during the summer months. Agriculture in the region is predominantly field crops like corn and wheat, with extensive tile drainage (~40% by field area, GRCA 2018) and fertilizer application in the late spring. River and in-lake, epilimnetic nutrient concentrations are reflective of these seasonal patterns. High nutrient concentrations in rivers and streams are typically observed in March and April (soluble reactive phosphorus: 10–150 $\mu g \cdot L^{-1}$; Ontario Provincial Water Quality Monitoring Network (station ID 16018407502)) with subsequent declines. In-lake, epilimnetic concentrations of soluble reactive phosphorus and total phosphorus in July have previously been reported at 0 and 13 $\mu g \cdot L^{-1}$, respectively, whereas nitrate and total nitrogen were substantially higher at 2.3 and 5.7 mg $N \cdot L^{-1}$, respectively (Guildford 2006).

Conestogo Lake, like many reservoirs in the area (Winter et al. 2011), is particularly prone to late-summer cyanobacterial blooms. Guildford et al. (2006) recorded cyanobacterial dominance (>50%) in the phytoplankton community in early September, the timing with which aligns with the GRCA's observational account over the last decade. (S. Cooke, personal communication 2018).

## Sample collection

We sampled a lacustrine (43.676518, −80.718752; max depth = 17 m) and transitional (43.708102, −80.712224; max depth = 9 m) site in Conestogo Lake once per week from 21 June to 17 August 2017. Water column profiles and samples for chemical analysis were collected at the lacustrine site on 21 June (day of year (DOY) 172) with biological sampling beginning on 5 July (DOY 186). Sampling in the transitional zone began on 5 July, 2 weeks after the extreme rainfall event (**Fig. 1a**). We measured water column profiles at 0.5 m increments using an EXO2 sonde (YSI, Yellow Springs, Ohio, USA) equipped with chlorophyll-a ($\mu g \cdot L^{-1}$), pH, temperature (°C), and dissolved oxygen (DO, $mg \cdot L^{-1}$) sensors. Photosynthetically active radiation (PAR) in the water column was also measured in 0.5 m increments using a LI-COR Underwater Quantum Sensor (LI-250A, LI-192, Lincoln, Nebraska, USA).

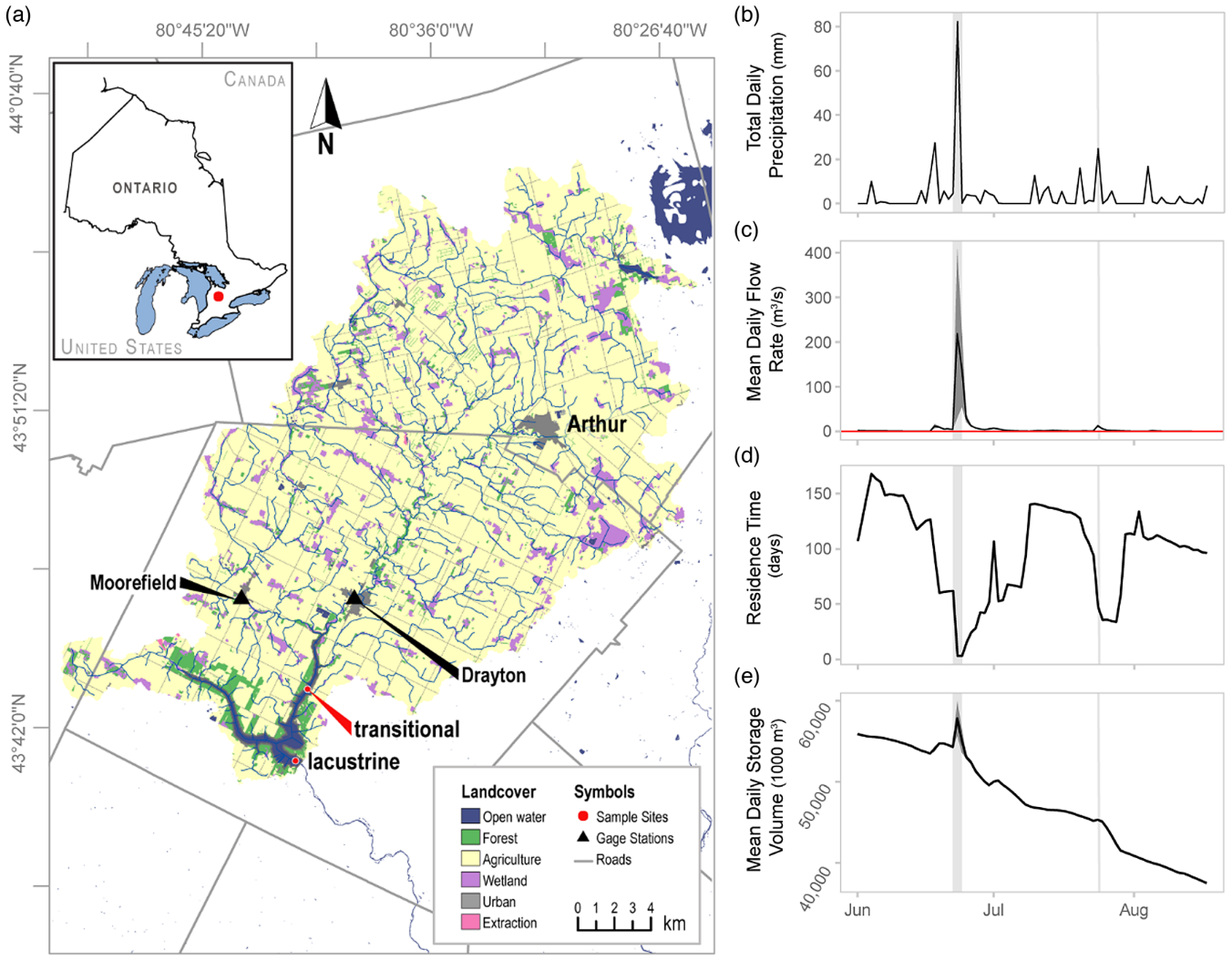


**Fig. 1.** Conestogo Lake (Mapleton Township, Ontario, Canada) and its associated watershed (a). Sampling began on 21 June 2017 (day of year (DOY) 172) in the lacustrine zone and on 5 July (DOY 186) in the transitional zone. Total daily precipitation (mm) measured in upper Conestogo watershed (b, gauge in Arthur, Ontario) was directly related to the Conestogo River mean daily flow rate (c, $n = 48$) into the reservoir (gauges in Drayton and Moorefield, Ontario) and the calculated reservoir residence time (d). The average flow rate during the drawdown period (May–September; red line, c) is typically near 0.01 $m^3 \cdot s^{-1}$. The extreme precipitation event beginning on 23 June (DOY 173; grey vertical bar) directly corresponds to in increased mean daily flow into the Conestogo Reservoir, increased reservoir storage (e), and reduced residence time. The dark grey area around the mean represents the standard deviations of daily measurements (flow, $n = 48$; storage, $n = 24$). A secondary rainfall event (~25 mm) on 24 July (DOY 205) also impacted flow rates into the reservoir. This figure contains information made available under GRCA's Open Data Licence v3.0 (a) and v2.0 (b–e). The map was produced by J. Atkins (Wilfrid Laurier University) using NAD 1983 Lambert Conformal Conic and GCS North American 1983 projection.

For all chemical analyses, discrete water samples were collected at 2 and 7 m below (lacustrine only) the water surface, and 0.5 m from the bottom using a Van Dorn bottle. Unfiltered whole water samples at each depth were portioned into acid-washed 50 mL centrifuge tubes for total phosphorus (TP, $\mu g \cdot L^{-1}$) and into a 125 mL dark bottle for phytoplankton enumeration (2 m only). Additional aliquots were field-filtered using a 0.45 µm syringe filter (Whatman®, Global Life Sciences Solutions, Marlborough, Massachusetts) for soluble reactive phosphorus (SRP, $\mu g \cdot L^{-1}$), total dissolved

phosphorus (TDP, $\mu g \cdot L^{-1}$), ammonium ($NH_4^+$, mg $N \cdot L^{-1}$), total dissolved nitrogen (TDN, mg $N \cdot L^{-1}$), anions ($NO_2^-$, $NO_3^-$, mg $N \cdot L^{-1}$; $Cl^-$, $SO_4^-$, $mg \cdot L^{-1}$), total dissolved iron (TDFe, $mg \cdot L^{-1}$), and cations ($Mg^{2+}$, $Ca^{2+}$, $Mn^+$ $mg \cdot L^{-1}$). All samples were transported on ice and chemical samples stored frozen until analysis at the University of Waterloo (Waterloo, Ontario) or Centre for Cold Regions and Water Science (Waterloo, Ontario).

Samples for total (i.e., intracellular and extracellular) metabolites were pooled from four discrete depths across the site-specific photic zone (2× Secchi depth). The method serves to sample the photic zone as a mechanism of estimating all possible toxins in the surface and near-surface waters. The estimated photic zone was split into four equal segments, sampled at each segmented depth using a Van Dorn bottle, then pooled in a bleach-sterilized bucket. For example, a Secchi depth measured at 1 m would be multiplied by two then divided by four to create four discrete samplings at 0.5, 1, 1.5, and 2 m. Each pooled sample was collected in an amber Nalgene polyethylene terephthalate glycol bottle to limit adsorption (Fisher reference: 322021-0125). All samples were stored frozen at −20 °C until analysis at the Université de Montréal (Montréal, Quebec).

## Chemical analyses

SRP, TDP, and TP concentrations were measured on a Cary 100 UV-Vis spectrophotometer (Santa Clara, California, USA) following off-line persulfate digestion (TP samples only) as per standard methods (Eaton et al. 1998). Each N parameter was analysed on a separate instrument with $NH_4^+$ and TDN analysed on a Westco Smartchem Analyzer (Unity Scientific, Milford, Massachusetts, USA) and Shimadzu TN-L analyser (Kyoto, Japan), respectively. Anion concentrations including $NO_2^-$ and $NO_3^-$ were measured on a Dionex Ion Chromatogram ICS-200 (Waltham, Massachusetts, USA) while cations and TDFe were measured on a Perkin Elmer Optima 8000 ICP-OES (Waltham, Massachusetts, USA). Total suspended solids (TSS; mg/L) were analysed as per Baulch et al. 2013.

## Phytoplankton identification and enumeration

Phytoplankton enumeration was completed by D. Findlay (Plankton-R-Us, Winnipeg, Manitoba, Canada, plankton-r-us.ca) as per Findlay and Kling (2003). Each sample was preserved with 4% Lugol's iodine, gravity concentrated 5-fold after 24 h, and stored at 4 °C for ~2 months until analysis. Enumeration was completed on an inverted microscope at 125×, 400×, and 1200× with phase contrast illumination using a modified Ütermohl technique (Nauwerk 1963) on 10 mL aliquots of preserved sample. Only cells with viable chloroplasts were enumerated. Cell counts were converted to milligrams of wet weight biomass ($mg \cdot m^{-3}$) by approximating cell volume, which were obtained by measurements of up to 50 cells of an individual species and applying the geometric formula best fitted to the shape of the cell (Vollenweider 1968). A specific gravity of 1 was assumed for cellular mass (D. Findlay, personal communication 2018).

## Cyanobacterial metabolite analysis

Samples were prepared and screened for each of 17 cyanobacterial secondary metabolites (**Table S1**) as per Fayad et al. (2015) via online solid phase extraction ultra-high performance liquid chromatography high-resolution mass spectrometry using standards purchased from Enzo Life Science, Abraxis, or Cyano Biotech GmbH. The limit of detection (LOD) and limit of quantification (LOQ) were calculated for each analyte (**Table S1**) and integrated into the data set for those values < LOD (i.e., left-censored values). Ninety percent of the toxin measurements were left-censored. Means and standard deviations presented in-text were calculated using the Kaplan–Meier method (*cenfit*) from the NADA package (Lee 2020) in R version 3.6.1 (R Core Team 2018).

## Environmental and dam-related data

Meteorological and other reservoir-related data for this study were obtained from the GRCA's online data portal (data.grandriver.ca/). Because GRCA data are provisional, all data were passed through quality assurance and quality checking metrics to check for outliers and missing data before proceeding with analysis. Spatial data were obtained from open source portals at the GRCA, the United States Geological Society (usgs.gov/), Statistics Canada (www12.statcan.gc.ca/), and the Ontario Ministry of Natural Resources (land-use; ontario.ca).

## Data analysis and statistics

All data analysis was completed in R version 3.6.1 (R Core Team 2018). Sonde-derived water column profiles as well as the discrete chemical profiles were constructed using a multilevel B-spline interpolation from the *MBA* package (Finley et al. 2017) and were adjusted to reflect the reservoir stage elevation at the time of sampling.

To compare phytoplankton community composition with environmental variables, we used principal components analysis (PCA) and redundancy analysis (RDA) including environmental variables from the epilimnion and 0.5 m above the sediment–water interface. Species biomass data were Hellinger transformed as recommended for species linear ordinations (Legendre and Gallagher 2001), which normalizes for both the site and species biomass needed for RDA. Only species that appear more than two times in the data set were included in these analyses. The environmental matrix included all chemical parameters at 2 m depth (epi) and those from 0.5 m above the sediment–water interface (sed), sonde-derived measurements for the epilimnion and hypolimnion (temperature, pH, DO), as well as physical lake parameters (thermocline depth and metalimnion layer depth; calculated using the *rLakeAnalyzer* package (Winslow et al. 2019)). We constructed PCA biplots with either species vectors that exceeded a cumulative goodness-of-fit of at least 0.6 in the ordination plane or significant environmental parameters. The higher the goodness-of-fit, the better the species is fitted on the corresponding axis. To test for the significance of environmental factors affecting the phytoplankton community, permutation tests (permutations = 999) on the models were completed using *anova.cca* from the package *vegan*. Epilimnetic chemistry, biomass, and toxin trends were analysed using repeated measures ANOVA (RM-ANOVA) with a generalized least squares model (*gls*) from the *nlme* package (Pinheiro et al. 2018) where time and site were fixed effects and the correlation matrix was selected based on Akaike Information Criterion. To account for temporal autocorrelation, we nested time within site. Finally, we tested for the correlation of biomass with toxin concentration (nondetects replaces with LOD) using Kendall's rho.

# Results

## Extreme rainfall disturbance in early summer

Record rainfall (daily range 40–120 mm) was recorded across the upper Conestogo watershed on 23 June 2017 (DOY 174) and led to widespread flooding. This event was the largest single rainfall in the Grand River Watershed since recording began in 1950 (GRCA 2017).

Mean daily flow rates into Conestogo Lake via the Conestogo River increased from 4.56 $m^3 \cdot s^{-1}$ to 219 $m^3 \cdot s^{-1}$ (max 521 $m^3 \cdot s^{-1}$), which consequently increased the total reservoir volume by 3.5 $Mm^3$, and is estimated to have replaced ~80% of the total reservoir volume (**Figs. 1b–1e**) (GRCA 2018). Reservoir residence time during this period was 6.04 d, as compared with the normal ranges between 26 and 119 d (mean = 43 d; GRCA 2018). Within several days, the reservoir storage and drawdown returned to levels targeted for regular reservoir operation.

Reservoir volume replacement restructured the physical water column. Both the transitional and lacustrine zones were well mixed, isothermal, and oxygenated immediately following the event (Fig. 2). Thermal stratification did not return to either location during the sampling period. Intermittent hypolimnetic hypoxia (DO < 2 $mg{\cdot}L^{-1}$) developed in the transitional zone while sustained hypoxia developed in the lacustrine within two weeks of the flood event (5 July, DOY 186). The Provincial Water Quality Monitoring Network (data.ontario.ca/dataset/provincial-stream-water-quality-monitoring-network) reported filtered reactive P concentrations at 6.5 and 10.5 $\mu g{\cdot}L^{-1}$ for the Conestogo River (station ID 16018407502) and Moorefield Creek (station ID 16018409102), respectively on 15 June 2017 (6 d prior to the event). Nitrate concentrations from the same stations were 0.517 and 1.47 mg $N{\cdot}L^{-1}$, respectively. Following the flooding event, lacustrine SRP, TDP, and TP increased between 2 and 33 times across the sampled depths (2m: SRP from 2.39 to 65.20 $\mu g{\cdot}L^{-1}$, TDP from 9.96 to 85.77 $\mu g{\cdot}L^{-1}$, TP from 14.99 to 103.48 $\mu g{\cdot}L^{-1}$; 7m: SRP from 2.27 to 73.98 $\mu g{\cdot}L^{-1}$, TDP from 9.69 to 92.69 $\mu g{\cdot}L^{-1}$, TP from 12.75 to 116.31 $\mu g{\cdot}L^{-1}$; bottom [16m]: SRP from 31.25 to 61.21 $\mu g{\cdot}L^{-1}$, TDP from 40.17 to 76.62 $\mu g{\cdot}L^{-1}$, TP from 43.89 to 118.78 $\mu g{\cdot}L^{-1}$; Figs. 2 and 3). Nitrogen concentrations at all measured depths were only marginally different postrainfall and maintained concentrations near 5.5 mg $N{\cdot}L^{-1}$ for $NO_3^-$ (mean prior =4.89 mg $N{\cdot}L^{-1}$; mean after = 5.45 $mg{\cdot}L^{-1}$) and TDN (mean prior = 5.63 mg $N{\cdot}L^{-1}$; mean after = 5.71 $mg{\cdot}L^{-1}$) (Fig. 2).

## Dynamics following early summer extreme rainfall event

Mean surface water temperatures (0–2 m) across the reservoir ranged from 21.2 to 25.5 °C. Nutrient concentrations (both N and P) were, on average, higher in the transitional zone than the lacustrine zone and significantly changed through time (Table 1; RM-ANOVA). Epilimnetic chlorophyll a, dissolved oxygen (DO), and temperature did not significantly change through time across sites. As predicted, the transitional zone had higher concentrations of suspended solids in the water column and lower light availability as compared with the lacustrine immediately following the reservoir disturbance (Fig. 4).

### Phytoplankton community composition

The transitional zone phytoplankton community was composed predominately of diatoms including *Stephanodiscus niagarae* (P5530) and *Cyclotella psuedostelligera* (P5508) and the dinoflagellate *Ceratium hirundenella* (P7644) with approximately five times more phytoplankton biomass in the transitional (total = 5742 $mg{\cdot}m^{-3}$ wet weight) than the lacustrine (total = 1113 $mg{\cdot}m^{-3}$ wet weight; 2 weeks postextreme event, Fig. 5a). In contrast with the transitional zone, the lacustrine zone contained high relative abundances of Cryptophytes including *Cryptomonas rostratiformis* (P6565), *C. erosa* (P6558), and *Rhodomonas minuta* (P6554) and Chrysophytes (*Ochromonas globose* (P4398)), all of which returned following the cyanobacterial bloom. Communities following the extreme rainfall event (DOY 186) were strongly associated with PAR and epilimnetic SRP, TDP, and TP. Communities in both zones gave way to cyanobacterial dominance (>50% of community by biomass, Figs. S1 and S2) 20–24 d following the flood with apparent changes to epilimnetic temperature and pH associated with temporal community shifts and increased presence of the filamentous nitrogen-fixer, *A. flos-aquae* (Fig. 6a; P1041).

### Cyanobacterial dynamics

Cyanobacterial bloom duration, measured as the period during which cyanobacterial biomass comprised >50% of the fractional biomass, persisted between 26 and 34 d and occurred 4–6 weeks earlier than has been previously documented (Guildford 2006; S. Cooke, personal communication 2018). Bloom initiation was 6 d earlier in the transitional zone as compared with the lacustrine. Mean total cyanobacterial biomass over the sampling campaign was $1550 \pm 2920$ $mg{\cdot}m^{-3}$ and

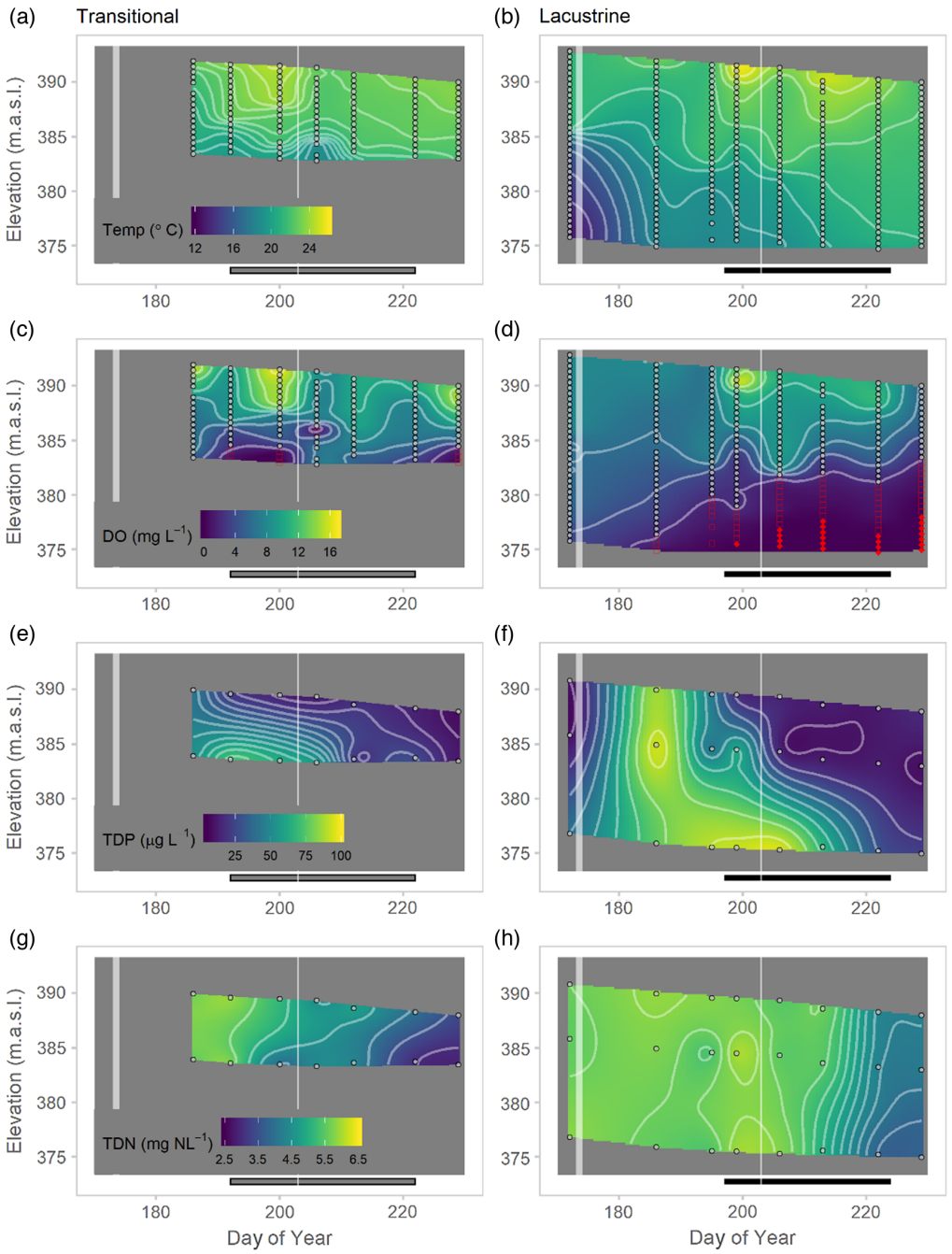


**Fig. 2.** Temperature (a and b, °C) and dissolved oxygen (DO; c and d, mg·L$^{-1}$) water column profiles collected at 0.5 m depth increments (grey points) in the transitional (a, c) and lacustrine (b, d) zones from 21 June 2017 (lacustrine only; day of year (DOY) 172) to 17 August (DOY 229). Hypoxic (red squares) zones were detected at all sites, but anoxia (red triangles) was only detected in the lacustrine zone. Total dissolved phosphorus (TDP) (e and f) and total dissolved nitrogen (TDN) (g and h) profiles collected at 2 and 7 m below (lacustrine only) the surface and 0.5 m from the bottom. Profile depths at each site were standardized to the dam stage elevation (meters above sea level (m.a.s.l.)) at the time of sampling. The grey regions in the *x*–*y* plane illustrate the interaction between time and reservoir depth at each site, where the *x*-axis zone indicates a later sampling date in the transitional and the *y*-axis grey zones illustrate differences in site depths with reference to the dam (max elevation = 393 m.a.s.l., dam outflow = 373.5 m.a.s.l.). The first white vertical bar corresponds to the record rainfall event on (23 June 2017; DOY 174) and the second to a 25 mm rainfall event on 24 July (DOY 205). The black horizontal bar corresponds to the bloom period in each of the two zones.

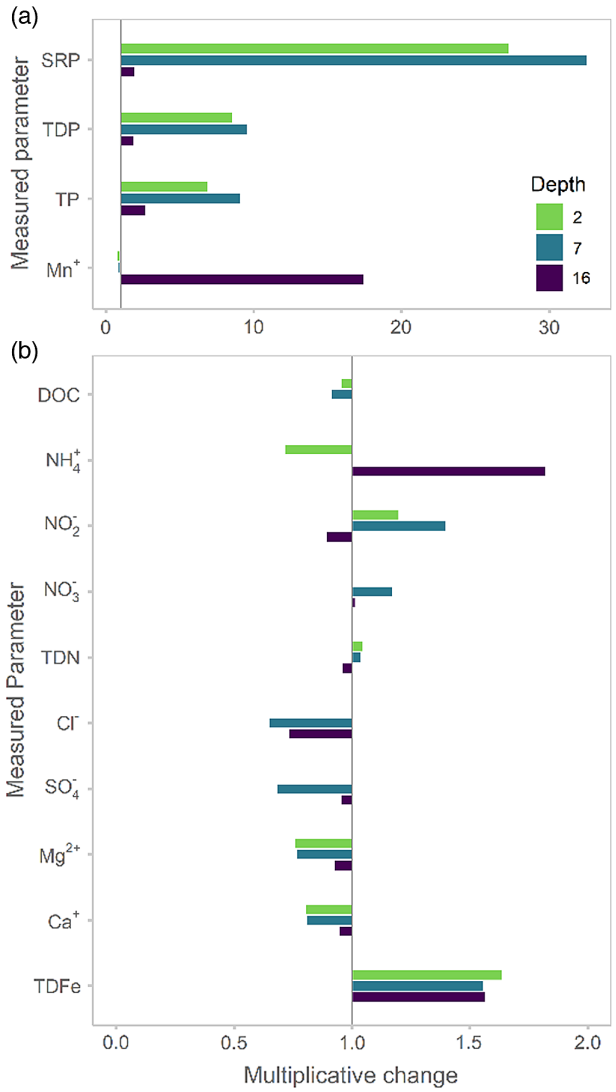


**Fig. 3.** Multiplicative changes in measured water chemistry prior to (21 June 2017, DOY 172) and after the early summer flood event (5 July 2017, day of year 186) in the lacustrine zone. Samples were collected at 2 m depth (purple), 7 m depth (blue), and 0.5 m from sediment–water interface (16 m; green) in the lacustrine zone. Values above 1 (black horizontal line) correspond to increased concentrations while those below 1 indicate reduced concentrations. Samples at 2 m for anions (b; ($NO_3^-$, $Cl^-$, $SO_4^-$)) were not analysed. SRP, soluble reactive phosphorus; TDP, total dissolved phosphorus; TP, total phosphorus; DOC, dissolved organic carbon; temp, water temperature; TDN, total dissolved nitrogen; TDFe, total dissolved iron.

591 ± 1290 mg·m$^{-3}$ in the transitional and lacustrine zones, respectively, and was significantly driven by an interaction between SRP and surface temperatures (RM-ANOVA, $F_{1,6} = 6.84$, $p = 0.0399$). There was no relationship between total cyanobacterial biomass and time or site (RM-ANOVA, $F_{1,10} = 0.086$, $p = 0.77$). *A. flos-aquae* was the dominant species and represented 95%–97% (by biomass) of the cyanobacterial fraction across all sites for the entirety of the sampling campaign. The highest measured *A. flos-aquae* biomass occurred on 19 July (DOY 200, 10 900 mg·m$^{-3}$, 4500 cells·mL$^{-1}$) in the transitional and near 25 July (DOY 206; 4710 mg·m$^{-3}$) in the lacustrine.

Table 1. Postflood mean (minimum – maximum) values for measured epilimnetic (2 m) characteristics in the transitional and lacustrine zones with RM-ANOVA *p* values.

| | Chl-a ($mg \cdot L^{-1}$) | DO ($mg \cdot L^{-1}$) | Temp (°C) | $NO_3$-N ($mg \cdot L^{-1}$) | TDN ($mg \cdot L^{-1}$) | SRP ($\mu g \cdot L^{-1}$) | TDP ($\mu g \cdot L^{-1}$) | PAR ($\mu mol \cdot s^{-1} \cdot m^{-2}$) |
|---|---|---|---|---|---|---|---|---|
| Transitional | 6.8 (1.6–14.0) | 10.6 (7.9–14.5) | 22.8 (21.7–24.0) | 4.82 (3.99–5.65) | 5.32 (4.24–5.86) | 13.66 (1.52–65.2) | 28.76 (11.62–85.77) | 42.6 (6.33–93.9) |
| Lacustrine | 5.4 (2.2–10.1) | 8.6 (5.6–11.0) | 22.3 (21.2–23.2) | 4.37 (3.34–5.63) | 4.74 (3.39–5.85) | 5.89 (1.56–24.61) | 18.53 (7.79–41.59) | 69.1 (16.0–155) |
| Intercept | **0.001** | **<0.001** | **<0.001** | **<0.001** | **<0.001** | **0.01** | **0.001** | **<0.001** |
| Time | 0.415 | 0.882 | 0.234 | **<0.001** | **<0.001** | **0.014** | **0.007** | **0.003** |
| Site | 0.586 | 0.204 | 0.244 | **0.001** | **0.004** | 0.196 | 0.206 | 0.064 |

**Note:** Bold values are significant ($p < 0.05$). Chl-a, chlorophyll a; DO, dissolved oxygen; temp, water temperature; $NO_3$, nitrate; TDN, total dissolved nitrogen; SRP, soluble reactive phosphorus; TDP, total dissolved phosphorus; PAR, photosynthetically active radiation.

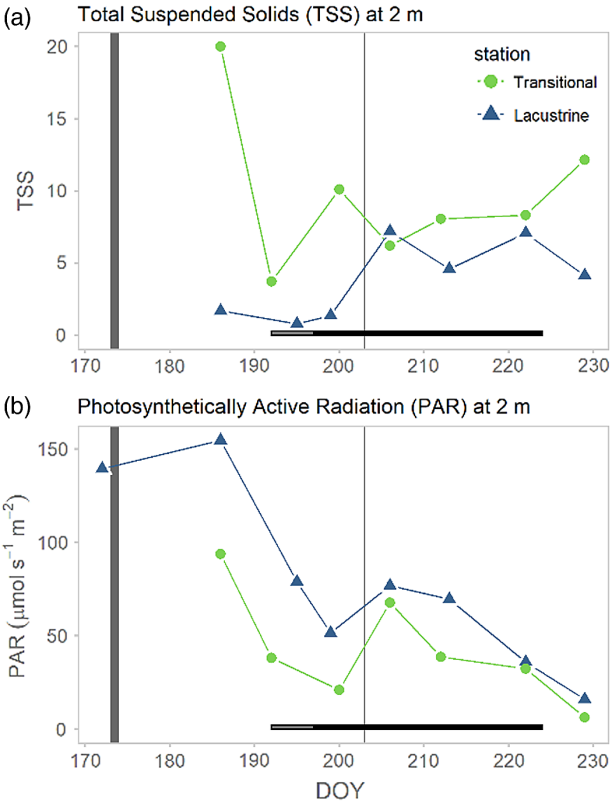


**Fig. 4.** Total suspended solids (TSS mg/L) (a) and light availability (b; photosynthetically active radiation (PAR) at 2 m in the transitional (green) and lacustrine (purple) zones. The horizontal bar corresponds to the cyanobacteria bloom period in the transitional (grey) and lacustrine (black) zones while the vertical bars are associated with the extreme rainfall event on 23 June (day of year (DOY) 174) and the late summer event on 24 July (DOY 205).

*Woronichinia compacta*, *A. (Dolichospermum) flos-aquae*, and *M. aeruginosa* were minor contributors (<5%) to cyanobacterial biomass while *A. (Dolichospermum) crassa*, *Planktolyngbya limnetica*, and *Pseudoanabaena* sp. were only observed once during the campaign at low biomass (<8 mg·m$^{-3}$). GRCA managers have visibly recorded cyanobacterial blooms dominated by an *Aphanizomenon* sp. in Conestogo Lake from late August through September (DOY ~220–250) since 2004 (S. Cooke, personal communication 2018).

## Cyanotoxin dynamics

Four of the 17 screened cyanobacterial metabolites were detected in Conestogo Lake. Detectable anabaenopeptin-A (AP-A), microcystin-LR (MC), -YR, and -RR were present in 87% of the samples ($n = 13$) but were only quantifiable in 73% ($n = 11$; **Table 2**). Total microcystin concentration did not exceed the recreational limit for total microcystins (20 000 ng·L$^{-1}$; Health Canada 2012) and was comparable with previously measured concentrations during the summer months (Yakobowski 2008). Metabolite type and concentration varied through time (RM-ANOVA, $F_{3,44} = 9.21$, $p = 0.001$) and were different between the two sites (RM-ANOVA, $F_{1,44} = 6.55$, $p = 0.014$). Quantifiable concentrations of all three microcystins were present in the transitional zone, whereas MC-LR and MC-YR were present in the lacustrine. MC-LR was the dominant microcystin variant across all sites with the highest quantified values (mean (SD) = 74.46 ± 156.5 ng·L$^{-1}$) in the transitional zone at peak *A. flos-aquae* and *M. aeruginosa* biomass (**Fig. 5b**, **Table 2**). Further, MC-YR in the lacustrine did

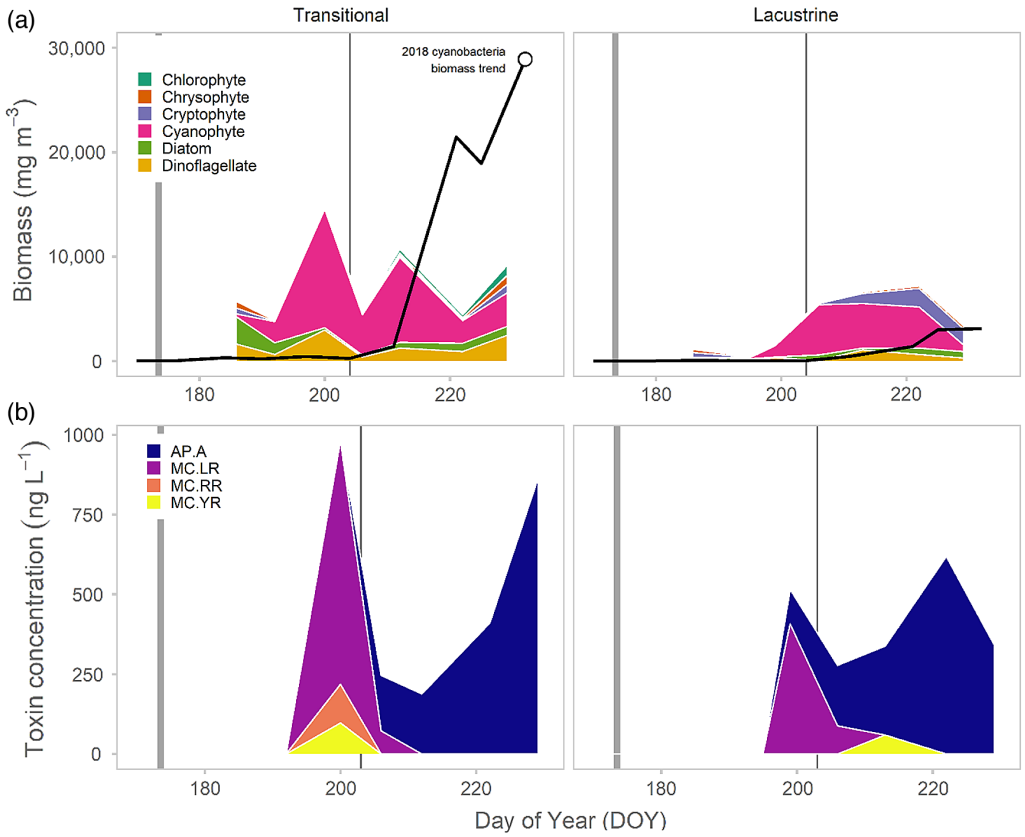


**Fig. 5.** Phytoplankton biomass (a) and cyanobacterial metabolite concentration trends (b; exceeding the limit of quantification) for anabaenopeptin-A (AP.A) and microcystin-LR (MC.LR), -YR (MC.YR), and -RR (MC.RR) in the transitional and lacustrine zones. The flood event beginning on 23 June (day of year (DOY) 174) and secondary event on 25 July (DOY 205) are noted by vertical bars. *Aphanizomenon flos-aquae* dominated (>50%) phytoplankton biomass in the transitional zone near 10 July 2017 (DOY 191) and in the lacustrine near 16 July 2017 (DOY 197). Only cyanobacterial species that were present in more than two samples are plotted above. Of the seven cyanobacterial species detected, various strains of *A. flos-aquae*, *A. flos-aquae (Dolichospermum flos-aquae)*, *M. aeruginosa*, and *W. compacta* have been documented as potential toxin producers. Typical bloom onset, as illustrated by the total cyanobacterial biomass from 2018 (black line) occurs between DOY 220–DOY 255 (Guildford 2006; S. Cooke, personal communication 2018).

not correspond with the MC-LR peak. High concentrations of AP-A were present in both zones (lacustrine = 201.5 ± 213.7 ng·L$^{-1}$; transitional = 240.9 ± 317.3 ng·L$^{-1}$) throughout the bloom period and, by the end of the sampling campaign, had entirely replaced microcystin variants.

MC-LR concentration was significantly correlated with the biomass of *M. aeruginosa* (Kendall rho = 0.76, $p = 0.03$). No other toxin was correlated with the biomass of any other observed cyanobacterial species.

## Dynamics following smaller mid-summer runoff event

A second, much smaller and transient increase in flow to the reservoir occurred on 24 July (DOY 205), associated with an ~25 mm rainfall event occurring during already wet conditions (Fig. 1). Effects of this event were much more muted. Overall, there was a slight decrease in surface water

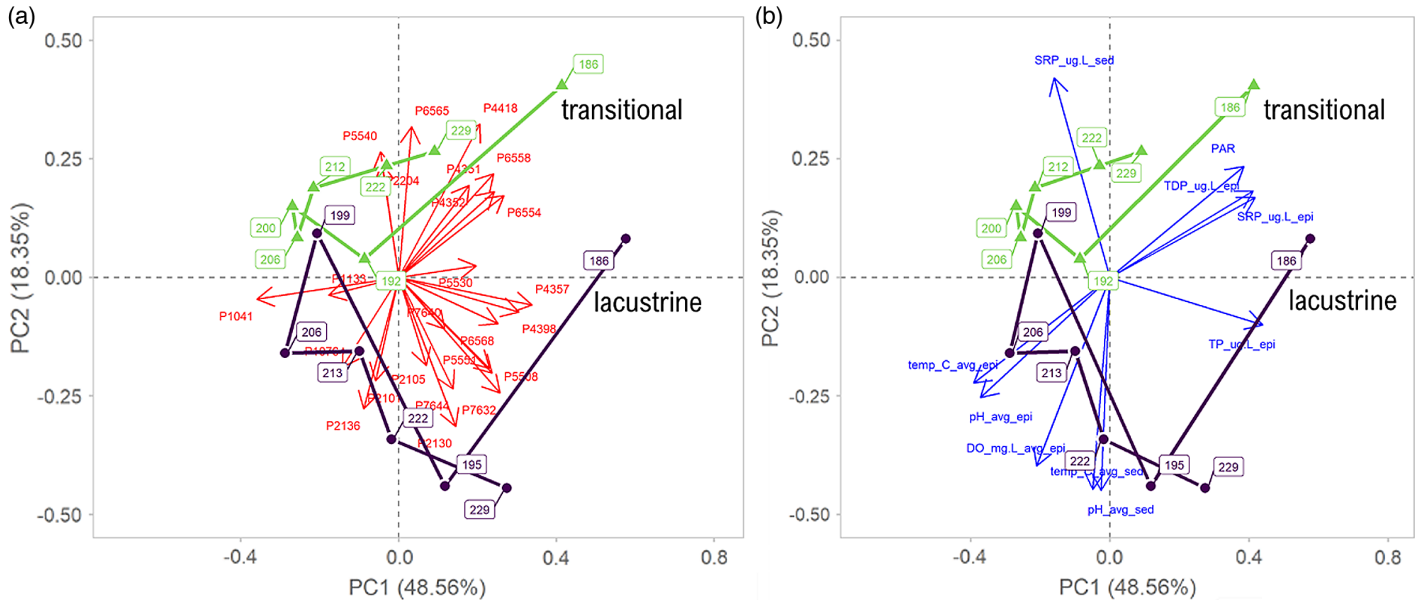


**Fig. 6.** Principal component analysis (scaling 1) of phytoplankton community, with the most influential phytoplankton species (a, goodness of fit > 0.6) and significant ($p < 0.05$) and weekly significant ($p < 0.1$) environmental variables (b). The length of the vector is proportional to the importance of the descriptor to the sites. The day of year for each community are in boxes and are linked through time for each reservoir zone (lacustrine (purple), transitional (green). Phytoplankton labels: P1041, *Aphanizomenon flos-aquae*; P2235, *Ankistrodesmus spiralis*; P6554, *Rhodomonas minuta*; P6558, *Cryptomonas erosa*; P4398, *Ochromonas globose*; P5515, *Fragilaria crotonensis*; P7644, *Ceratium hirundenella*. Environmental labels: SRP_ug.L_epi, epilimnetic soluble reactive phosphorus; SRP_ug.L_epi, sedimentary soluble reactive phosphorus; TDP_ug.L_epi, epilimnetic total dissolved phosphorus; TP_ug.L_epi, epilimnetic total phosphorus; PAR, photosynthetically active radiation; DO_mg.L_avg_epi, epilimnetic dissolved oxygen; pH_avg_epi, epilimnetic pH; pH_avg_sed, sedimentary pH; temp_C_avg_epi, epilimnetic temperature; temp_C_avg_sed, sedimentary temperature.

temperatures and decrease in the extent of oxygen supersaturation in both reservoir zones, with minimal effects on nutrients (Fig. 2). TSS increased slightly in the lacustrine zone and decreased in the transitional zone, suggesting the event was not of sufficient magnitude to lead to substantive additional erosion in the upstream catchment. Light irradiation increased in both areas (Fig. 4). In the transitional zone, this change was concurrent with a 66% decrease in total phytoplankton biomass and ~50% decrease in TSS while the lacustrine showed increases in both during this period (Figs. 4 and 5). Though the phytoplankton community composition in the transitional zone did not change, the lacustrine showed a marked increase in the cryptophyte *Katablepharis ovalis* (P6568) for the rest of the sampling period. Total cyanobacterial toxin concentrations declined by ~75% in the transitional zone, while more muted declines were apparent in the lacustrine. All MC variants were replaced with AP-A as the dominant metabolite at all sites by 25 July (DOY 206).

## Discussion and conclusions

Globally, increases in extreme rainfall events are predicted to outpace changes in total precipitation (Allen and Ingram 2002; IPCC 2007; Soulis et al. 2016). The impacts of extreme rainfall on cyanobacterial blooms are inherently complex (Reichwaldt and Ghadouani 2012; Wood et al. 2017) with the overall effect regulated by parameters including intensity, volume of water inflow, and timing with respect to seasonality (reviewed in Reichwaldt and Ghadouani 2012). The limited studies investigating such extreme rainfall events on cyanobacterial bloom development have identified changes to flushing rates, water column mixing, and nutrient inputs from rainfall events as the main abiotic factors

Table 2. Quantified cyanobacterial metabolites across sampling sites as measured by LC-HMRS

| | | Cyanobacterial secondary metabolites | | | |
|---|---|---|---|---|---|
| Site | Date | AP-A | MC-LR | MC-RR | MC-YR |
| Lacustrine | 21 June | — | — | — | — |
| | 5 July | — | — | — | *33.3 (16.1)* |
| | 14 July | *23.7 (4.9)* | — | — | *20.6 (29.1)* |
| | 18 July | 109.3 (78.6) | 406.9 (18.1) | — | — |
| | 25 July | 189.7 (35.6) | 88.2 (6.2) | *35.5 (9.2)* | *20.0 (28.2)* |
| | 1 August | 278.8 (27.4) | 16.8 (10.6) | — | 59.2 (16.5) |
| | 10 August | 619.3 (141.0) | — | — | *19.4 (1.3)* |
| | 17 August | 344.0 (50.3) | — | — | — |
| Transitional | 5 July | — | — | — | — |
| | 11 July | *18.6 (26.3)* | — | — | — |
| | 19 July | — | 763.6 (154.2) | 121.0 (1.6) | 97.3 (36.2) |
| | 25 July | 174.3 (34.9) | 72.1 (23.3) | *27.6 (2.7)* | — |
| | 31 July | 188.6 (108.5) | — | — | — |
| | 10 August | 411.0 (30.6) | — | — | — |
| | 17 August | 856.8 (37.2) | — | — | — |

**Note:** Cyanobacterial metabolite concentrations across sampling sites as measured by liquid chromatography high-resolution mass spectrometry (LC-HMRS). Values that exceeded the limit of quantification (LOQ) presented as mean $ng{\cdot}L^{-1}$ (standard deviation $ng{\cdot}L^{-1}$), those in italics exceeded the limit of detection (LOD) but not the limit of quantification, and those with "—" were <LOD. Reported means and standard deviations are inclusive of <LOD data (left-censored data) calculated with the Kaplan–Meier method. The metabolites MC-LA, -LY, -LW, -LF, -HiIR, -HtyR, anatoxin, homoanatoxin, cylindrospermopsin, and cyanopeptolin A were not detected in samples. AP-A, anabaenopeptin A; MC-, microcystin.

affecting cyanobacteria and phytoplankton communities (Bouvy et al. 2003; Reichwaldt and Ghadouani 2012)—all factors that appeared to impact the bloom dynamics in Conestogo Lake.

The record rainfall event effectively created a new, early-summer high-P regime as a result of the significant influx arriving from the Conestogo River and a near-complete replacement of the reservoir volume. Epilimnetic SRP concentrations in Conestogo Lake have ranged between 0 and 1.8 $\mu g{\cdot}L^{-1}$, whereas TDP and TP range between 8 and 15 $\mu g{\cdot}L^{-1}$ (Guildford 2006). During this event, epilimnetic SRP concentrations increased by ~7–27 times (from ~2 to 65 $\mu g{\cdot}L^{-1}$). Substantial increases in P loading, such as these, are common following heavy rainfall, particularly if they are preceded by warm, dry periods (Jones and Poplawski 1998; Lisboa et al. 2020). For example, in Australian reservoirs, a 440 mm rainfall in a 3-d period resulted in an input equivalent to 400% of the average annual in-lake P mass (Jones and Poplawski 1998). In our study system, the upper Conestogo watershed is predominantly Tavistock Till, which is particularly prone to erosion and serves as a key mechanism for particulate P transport (Loomer and Cooke 2003; Macrae et al. 2007). High flow events can also be important to transport of soluble P species, as P is desorbed from particulate forms or released from soils (Lisboa et al. 2020).

Though surface water temperatures remained similar following the June extreme rainfall event, the bottom sediments warmed from 13 to 18 °C. While we cannot isolate the effects of thermal and biogeochemical changes in bloom initiation, we note that in-lake nitrogen concentrations appear to have changed little as a result of the flooding despite the low concentrations (<1 mg $NO_3$-N·$L^{-1}$) in the upper Conestogo River preceding the event. This catchment has chronic high N concentrations (3–5 mg $NO_3$-N·$L^{-1}$), associated with long-term intensive agricultural usage within the catchment (Guildford 2006; Irvine et al. 2019). The lack of change in N suggests that it was not likely to be the key factor leading to early bloom initiation as previously noted (Guildford 2006). Iron too has been postulated as a key nutrient to support cyanobacterial growth and bloom induction (Molot et al. 2014). Although iron speciation was not monitored here, changes in total dissolved iron are likely to have been more associated with the traditional bloom period rather than the extreme event.

It appears that the excessive supply of P initiated the development of the observed weakly toxic early-summer cyanobacterial bloom (**Figs. 5** and **6**). Typically, N-fixing *A. flos-aquae* dominated blooms do not develop in the Conestogo Reservoir until late summer (S. Cooke, personal communication; Guildford 2006), ~35–40 d after our documented extreme event when typical in-lake N concentrations are much lower (Guildford 2006). The significant growth response by *A. flos-aquae*, as compared with other cyanobacteria, may have been in part driven by cooler water temperatures. *Aphanizomenon* species have lower temperature optima than other cyanobacteria (Konopka and Brock 1978) thereby potentially providing a competitive advantage over other species. Additionally, substantial *Aphanizomenon* akinete seeding from the sediments could have been flushed into the transitional zone water column by the increased river flows. Akinete populations have been postulated to act as an inoculum for summer blooms (Cirés et al. 2013). The bloom originating in the transitional zone was not only initiated a week earlier than in the lacustrine, but it was also sustained through the typical bloom period in September (S. Cooke, personal communication 2018; Guildford 2006), highlighting the potential for elongation of the bloom season and risk associated with extreme rainfall events. However, the magnitude of the transitional bloom was directly influenced by the mid-summer rainfall event, which flushed both biomass and toxins. The event was not of sufficient volume to have similar effects on the deeper, larger volume lacustrine zone.

The environmental factors driving toxin production and their seasonal dynamics are quite complex. We detected low quantities (<1000 ng·$L^{-1}$) of three MC variants, MC-LR, -YR, and -RR, in the early summer cyanobacterial bloom that dissipated following the mid-summer event. The total concentration of microcystins never exceeded the recreational limit (20 000 ng·$L^{-1}$; Health Canada 2012). Of these, only MC-LR was significantly correlated with the low biomass of a single taxa (*M. aeruginosa*). However, because it difficult to assign strong relationships between the toxins and cyanobacterial species without direct molecular studies (Vezie et al. 1998), it remains possible that there could be the presence of a rare, toxin-producing species or strain or multiple taxa involved in toxin production.

MC variants are not the only cyanobacterial compounds capable of impacting human health. Several studies using cyanobacterial extracts have reported harmful and (or) toxic effects that could not be explained solely by microcystin concentration or presence, suggesting the possibility of other toxic compounds (Keil et al. 2002; Teneva et al. 2005; Baumann and Jüttner 2008; Smutná et al. 2014; Lenz et al. 2019). Although not often reported, improved analytical techniques have identified numerous other bioactive compounds such as cyanopeptolins and anabaenopeptins that are both detectable in freshwaters and often produced simultaneously with microcystin variants (Harada et al. 1995; Welker and Von Döhren 2006; Gkelis et al. 2015; Beversdorf et al. 2017, 2018) at similar or greater levels (Janssen 2019). For example, Beversdorf et al. (2017) reported an average of 0.65 µg·$L^{-1}$ total microcystin in Lake Koshkonong, Wisconsin, while anabaenopeptin-B and -F were

measured at 6.56 $\mu g \cdot L^{-1}$ combined. Though there are no case studies of human toxicity caused by anabaenopeptins, the compound inhibits carboxypeptidase A, and like microcystin, also inhibits protein phosphatases with slightly overlapping inhibitory concentration ranges (Honkanen et al. 1990; Sano et al. 2001; Spoof et al. 2016). The concentrations of these toxins that could affect human health are unknown, which has prevented the development of recreational and drinking water regulations and (or) advisories for these potentially toxic compounds. Like some microcystins, the ecological effects of anabaenopeptins may be observed at relatively low concentrations. A recent study by Lenz et al. (2019) reported induced toxicity by low concentrations (10 $\mu g \cdot L^{-1}$) of anabaenopeptins, including AP-A, on the nematode *Caenorhabditis elegans* resulting in reduced reproduction, reduced lifespan, and delayed hatching. Though compounds like AP-A have been previously considered nontoxic, they may represent a new class of emerging toxins, whose potential impacts to human health and toxicity to aquatic organisms require immediate attention and, therefore, inclusion in risk assessment for lake mitigation and monitoring programs. Though the present study concluded prior to the peak bloom season in late August to September, GRCA managers took note of the sizable cyanobacteria biomass and issued public health alerts (S. Cooke, personal communication 2018, CTV News 2017). We recognize this is as a limitation in our study as the additional information from the traditional bloom period could have aided in further understanding to the effects of extreme events.

Global bloom incidence has been associated with elevated nutrient loads and with warming (Paerl and Otten 2016; Ho and Michalak 2020). However, more attention is needed to understand the role of extreme events in altering bloom risk, how these events may differ in their seasonal impacts, and on spatially complex but crucial water resources, such as reservoirs. The environmental factors driving cyanobacterial blooms are inherently complex and dynamic, making predictions about toxicity and impact on end-user health and safety difficult to obtain across diverse ecosystems. Extreme disturbance events, like the early summer event described here, will only make that task more difficult since they are not only predicted to increase but will also likely mask historical drivers of changes in bloom risk. Managers cannot effectively manage a future ecosystem based on averages of the past. Instead, a holistic understanding of multiple drivers of cyanobacterial bloom risk, accounting for both extreme events, and reservoir structure is required. Within this region, we hypothesize that early season events have the greatest potential to worsen bloom risk by extending the bloom season as shown here. Later season events may lead to increased annual nutrient loads but may also flush existing blooms, especially in the narrow sections of the transitional zones.

## Acknowledgements

Funding for this work was provided by the Canada First Research Excellence Fund program. This was a part of the Global Water Futures Initiative FORMBLOOM: FORecasting tools and Mitigation options for diverse BLOOM-affected lakes as well as the ATRAPP project (Algal Blooms, Treatment, Risk Assessment, Prediction and Prevention through Genomics) from Genome Canada and Genome Québec. We thank S. Cooke, D. McFadden, and the Grand River Conservation Authority for their cooperation and knowledgeable insight; R. Elgood, E. McQuay, T. Cornell, B. Gruber, S. Sine, and M. Soares-Paquin for assistance with sample collection and analysis; J. Atkins for her GIS assistance and map production; and the members of the Venkiteswaran and Schiff lab groups for their reviews of manuscript drafts and friendly discussion.

## Author contributions

MLL, HMB, SLS, DFS, SS, and JJV conceived of the ideas and designed methodology. MLL, DFS, and SS collected the data. MLL analysed the data and lead the writing of the manuscript. MLL, HMB, SLS, DFS, SS, and JJV contributed critically to the drafts and gave final approval for publication.

## Competing interests

The authors have declared that no competing interests exist.

## Data availability statement

Data and code that support the analysis and findings in this study are available in figshare at doi/10.6084/m9.figshare.7811963.

## Supplementary material

The following Supplementary Material is available with the article through the journal website at doi:10.1139/facets-2020-0022.

Supplementary Material 1

## References

Allen MR, and Ingram WJ. 2002. Constraints on future changes in climate and the hydrologic cycle. Nature, 419(6903): 224–232. DOI: 10.1038/nature01092

Baulch HM, Futter MN, Jin L, Whitehead PG, Woods DT, Dillon PJ, et al. 2013. Phosphorus dynamics across intensively monitored subcatchments in the Beaver River. Inland Waters, 3(2): 187–206. DOI: 10.5268/IW-3.2.530

Baumann HI, and Jüttner F. 2008. Inter-annual stability of oligopeptide patterns of Planktothrix rubescens blooms and mass mortality of Daphnia in Lake Hallwilersee. Limnologica, 38(3–4): 350–359. DOI: 10.1016/j.limno.2008.05.010

Beversdorf LJ, Rude K, Weirich CA, Bartlett SL, Seaman M, Kozik C, et al. 2018. Analysis of cyanobacterial metabolites in surface and raw drinking waters reveals more than microcystin. Water Research, 140: 280–290. DOI: 10.1016/j.watres.2018.04.032

Beversdorf LJ, Weirich CA, Bartlett SL, and Miller TR. 2017. Variable cyanobacterial toxin and metabolite profiles across six eutrophic lakes of differing physiochemical characteristics. Toxins, 9(62): 1–21. DOI: 10.3390/toxins9020062

Bouvy M, Nascimento SM, Molica RJR, Ferreira A, Huszar V, and Azevedo SMFO. 2003. Limnological features in Tapacurá reservoir (northeast Brazil) during a severe drought. Hydrobiologia, 493: 115–130. DOI: 10.1023/A:1025405817350

Bush E, and Lemmen DS (*Editors*). 2019. Canada's changing climate report. Government of Canada, Ottawa, Ontario.

Chorus I, and Bartram J (*Editors*). 1999. Toxic cyanobacteria in water: a guide to their public health consequences, monitoring and management. Vol. 31. E & FN Spon, London, UK and New York, New York. DOI: 10.1161/ATVBAHA.111.231050

Chorus I, Falconer IR, Salas HJ, and Bartram J. 2000. Health risks caused by freshwater cyanobacteria in recreational waters. Journal of Toxicology and Environmental Health, Part B, 3(4): 323–347. PMID: 11055209 DOI: 10.1080/109374000436364

Cirés S, Wörmer L, Agha R, and Quesada A. 2013. Overwintering populations of *Anabaena*, *Aphanizomenon* and *Microcystis* as potentia inocula for summer blooms. Journal of Plankton Research, 35(6): 1254–1266. DOI: 10.1093/plankt/fbt081

Codd GA. 2000. Cyanobacterial toxins, the perception of water quality, and the prioritisation of eutrophication control. Ecological Engineering, 16(1): 51–60. DOI: 10.1016/S0925-8574(00)00089-6

CTV News. 2017. GRCA warns blue-green algae found in the water at three local lakes. CTV News, Kitchener, Ontario [online]: Available from kitchener.ctvnews.ca/grca-warns-blue-green-algae-found-in-the-water-at-three-local-lakes-1.3591815.

Easterling DR, Kunkel KE, Arnold JR, Knutson T, LeGrande AN, Leung LR, et al. 2017. Precipitation change in the United States. Climate Science Special Report: Fourth National Climate Assessment. U.S. Global Change Research Program, Washington, D.C. DOI: 10.7930/J0H993CC

Eaton AD, Clesceri LS, Greenberg AE, and Franson MAH (*Editors*). 1998. 4500-P phosphorus. *In* Standard methods for the examination of water and wastewater. 20th ed. American Public Health Association, Washington, D.C.

Fayad PB, Roy-Lachapelle A, Duy SV, Prévost M, and Sauvé S. 2015. On-line solid-phase extraction coupled to liquid chromatography tandem mass spectrometry for the analysis of cyanotoxins in algal blooms. Toxicon, 108: 167–175. PMID: 26494036 DOI: 10.1016/j.toxicon.2015.10.010

Findlay DL, and Kling HJ. 2003. Protocols for measuring biodiversity: phytoplankton in freshwater. Department of Fisheries and Oceans, Winnipeg, Manitoba [online]: Available from ec.gc.ca/Publications/default.asp?lang=En&xml=4F5B7AEF-0B67-4D81-8F3F-62C103C5C9A6.

Finley A, Banerjee S, and Hjelle Ø. 2017. MBA: multilevel B-spline approximation [online]: Available from cran.r-project.org/package=MBA.

Gkelis S, Lanaras T, Sivonen K, and Taglialatela-Scafati O. 2015. Cyanobacterial toxic and bioactive peptides in freshwater bodies of Greece: Concentrations, occurrence patterns, and implications for human health. Marine Drugs, 13(10): 6319–6335. DOI: 10.3390/md13106319

Grand River Conservation Authority (GRCA). 2017. Record rainfall flood June 2017 [online]: Available from grandriver.ca/en/our-watershed/Record-Rainfall-Flood-June-2017.aspx.

Grand River Conservation Authority (GRCA). 2018. Belwood and Conestogo water management reservoirs: an assessment of surface and groundwater conditions DRAFT January 2018.

Guildford SJ. 2006. Factors controlling cyanobacteria blooms in three grand river basin reservoirs during 2005. Report to the Grand River Conservation Authority.

Harada K, Fujii K, Shimada M, Suzuki M, Sano H, Adachi K, et al. 1995. Two cyclic peptides, anabaenopeptins, a third group of bioactive compounds from the cyanobacterium Anabaena flos-aquae NRC 525-17. Tetrahedron Letters, 36(9): 1511–1514. DOI: 10.1016/0040-4039(95)00073-L

Health Canada. 2012. Guidelines for Canadian recreational water quality. 3rd ed. Health Canada, Ottawa, Ontario [online]: Available from canada.ca/en/health-canada/services/publications/healthy-living/guidelines-canadian-recreational-water-quality-third-edition.html.

Ho JC, and Michalak AM. 2020. Exploring temperature and precipitation impacts on harmful algal blooms across continental U.S. lakes. Limnology and Oceanography, 65: 992–1009. DOI: 10.1002/lno.11365

Ho JC, Michalak AM, and Pahlevan N. 2019. Widespread global increase in intense lake phytoplankton blooms since the 1980s. Nature, 574(7780): 667–670. PMID: 31610543 DOI: 10.1038/s41586-019-1648-7

Honkanen RE, Zwiller E, Mooren RE, Daily SL, Khatra BS, Dukelow M, et al. 1990. Characterization of Microcystin- LR, a potent inhibitor of type 1 and type 2A protein phosphatases. Biological Chemistry, 265(32): 19401–19404.

IPCC. 2007. Climate Change 2007: the scientific basis. Contribution of Working Group I to the Fourth Assessment Report of the Intergovernmental Panel on Climate Change. Cambridge University Press, New York, New York.

Irvine C, Macrae M, Morison M, and Petrone R. 2019. Seasonal nutrient export dynamics in a mixed land use subwatershed of the Grand River, Ontario, Canada. Journal of Great Lakes Research, 45(6): 1171–1181. DOI: 10.1016/j.jglr.2019.10.005

Jacobsen BA, and Simonsen P. 1993. Disturbance events affecting phytoplankton biomass, composition and species diversity in a shallow, eutrophic, temperate lake. Hydrobiologia, 249: 9–14. DOI: 10.1007/BF00008838

Janssen EM-L. 2019. Cyanobacterial peptides beyond microcystins – A review on co-occurrence, toxicity, and challenges for risk assessment. Water Research, 151: 488–499. DOI: 10.1016/j.watres.2018.12.048

Jöhnk KD, Huisman J, Sharples J, Sommeijer B, Visser PM, and Strooms JM. 2008. Summer heatwaves promote blooms of harmful cyanobacteria. Global Change Biology, 14(3): 495–512. DOI: 10.1111/j.1365-2486.2007.01510.x

Jones GJ, and Poplawski W. 1998. Understanding and management of cyanobacterial blooms in sub-tropical reservoirs of Queensland, Australia. Water Science and Technology, 37(2): 161–168. DOI: 10.2166/wst.1998.0130

Keil C, Forchert A, Fastner J, Szewzyk U, Rotard W, Chorus I, Krätke I. 2002. Toxicity and microcystin content of extracts from a Planktothrix bloom and two laboratory strains. Water Research, 36(8): 2133–2139. DOI: 10.1016/S0043-1354(01)00417-1

Kimmel BL, and Groeger AW. 1984. Factors controlling primary production in lakes and reservoirs: a perspective. Lake and Reservoir Management, 1(1): 277–281. DOI: 10.1080/07438148409354524

Konopka A, and Brock TD. 1978. Effect of temperature on blue-green algae (cyanobacteria) in Lake Mendota. Applied and Environmental Microbiology, 36: 572–576. PMID: 16345318 DOI: 10.1128/AEM.36.4.572-576.1978

Kossin JP, Hall T, Knutson T, Kunkel KE, Trapp RJ, Waliser DE, et al. 2017. Extreme storms. *In* Climate Science Special Report: Fourth National Climate Assessment. Vol. I. *Edited by* DJ Wuebbles, DW Fahey, KA Hibbard, DJ Dokken, BC Stewart, and TK Maycock. U.S. Global Change Research Program, Washington, D.C.

Lee L. 2020. NADA: nondetects and data analysis for environmental data.

Legendre P, and Gallagher ED. 2001. Ecologically meaningful transformations for ordination of species data. Oecologia, 129(2): 271–280. PMID: 28547606 DOI: 10.1007/s004420100716

Lenz KA, Miller TR, and Ma H. 2019. Anabaenopeptins and cyanopeptolins induce systemic toxicity effects in a model organism the nematode Caenorhabditis elegans. Chemosphere, 214: 60–69. DOI: 10.1016/j.chemosphere.2018.09.076

Lisboa MS, Schneider RL, Sullivan PJ, and Walter MT. 2020. Drought and post-drought rain effect on stream phosphorus and other nutrient losses in the Northeastern USA. Journal of Hydrology: Regional Studies, 28: 100672. DOI: 10.1016/j.ejrh.2020.100672

Loomer HA, and Cooke SE. 2003. Water quality in the Grand River watershed. Grand River Conservation Authority, Cambridge, Ontario.

Macrae ML, English MC, Schiff SL, and Stone M. 2007. Intra-annual variability in the contribution of tile drains to basin discharge and phosphorus export in a first-order agricultural catchment. Agricultural Water Management, 92(3): 171–182. DOI: 10.1016/j.agwat.2007.05.015

McDermid J, Fera S, and Hogg A. 2015. Climate change projections for Ontario: an updated synthesis for policymakers and planners. Climate Change Research Report CCRR-44. Ontario Ministry of Natural Resources and Forestry, Science and Research Branch, Peterborough, Ontario.

Mitrovic SM, Oliver RL, Rees C, Bowling LC, and Buckney RT. 2003. Critical flow velocities for the growth and dominance of *Anabaena circinalis* in some turbid freshwater rivers. Freshwater Biology, 48(1): 164–174. DOI: 10.1046/j.1365-2427.2003.00957.x

Molot LA, Watson SB, Creed IF, Trick CG, McCabe SK, Verschoor MJ, et al. 2014. A novel model for cyanobacteria bloom formation: the critical role of anoxia and ferrous iron. Freshwater Biology, 59(6): 1323–1340. DOI: 10.1111/fwb.12334

Nauwerk A. 1963. Die Beziehungen zwischen Zooplankton und Phytoplankton im See Erken. Symbolae Botanicae Upsalienses, 17(5): 1–163.

O'Neil JM, Davis TW, Burford MA, and Gobler CJ. 2012. The rise of harmful cyanobacteria blooms: the potential roles of eutrophication and climate change. Harmful Algae, 14: 313–334. DOI: 10.1016/j.hal.2011.10.027

O'Reilly CM, Sharma S, Gray DK, Hampton SE, Read JS, Rowley RJ, et al. 2015. Rapid and highly variable warming of lake surface waters around the globe. Geophysical Research Letters, 42(24): 10,773–10,781. DOI: 10.1002/2015GL066235

Orihel DM, Bird DF, Brylinsky M, Chen H, Donald DB, Huang DY, et al. 2012. High microcystin concentrations occur only at low nitrogen-to-phosphorus ratios in nutrient-rich Canadian Lakes. Canadian Journal of Fisheries and Aquatic Sciences, 69(9): 1457–1462. DOI: 10.1139/f2012-088

Paerl HW, and Huisman J. 2009. Climate change: a catalyst for global expansion of harmful cyanobacterial blooms. Environmental Microbiology Reports, 1(1): 27–37. PMID: 23765717 DOI: 10.1111/j.1758-2229.2008.00004.x

Paerl HW, and Otten TG. 2016. Duelling 'CyanoHABs': unravelling the environmental drivers controlling dominance and succession among diazotrophic and non-$N_2$-fixing harmful cyanobacteria. Environmental Microbiology, 18(2): 316–324. PMID: 26310611 DOI: 10.1111/1462-2920.13035

Paerl HW, Gardner WS, Havens KE, Joyner AR, McCarthy MJ, Newell SE, et al. 2016. Mitigating cyanobacterial harmful algal blooms in aquatic ecosystems impacted by climate change and anthropogenic nutrients. Harmful Algae, 54: 213–222. PMID: 28073478 DOI: 10.1016/j.hal.2015.09.009

Paerl HW, Hall NS, Hounshell AG, Luettich RA, Rossignol KL, Osburn CL, et al. 2019. Recent increase in catastrophic tropical cyclone flooding in coastal North Carolina, USA: long-term observations suggest a regime shift. Scientific Reports, 9(1): 10620. PMID: 31337803 DOI: 10.1038/s41598-019-46928-9

Pick FR. 2016. Blooming algae: a Canadian perspective on the rise of toxic cyanobacteria. Canadian Journal of Fisheries and Aquatic Sciences, 73(7): 1149–1158. DOI: 10.1139/cjfas-2015-0470

Pinheiro J, Bates D, DebRoy S, Sarkar D, and R Core Team. 2018. nlme: linear and nonlinear mixed effects models [online]: Available from cran.r-project.org/package=nlme.

R Core Team. 2018. R: a language and environment for statistical computing. R Foundation for Statistical Computing, Vienna, Austria [online]: Available from r-project.org/.

Reichwaldt ES, and Ghadouani A. 2012. Effects of rainfall patterns on toxic cyanobacterial blooms in a changing climate: between simplistic scenarios and complex dynamics. Water Research, 46(5): 1372–1393. PMID: 22169160 DOI: 10.1016/j.watres.2011.11.052

Richardson D, Melles S, Pilla R, Hetherington A, Knoll L, Williamson C, et al. 2017. Transparency, geomorphology and mixing regime explain variability in trends in lake temperature and stratification across northeastern North America (1975–2014). Water, 9(6): 442. DOI: 10.3390/w9060442

Sano T, Usui T, Ueda K, Osada H, and Kaya K. 2001. Isolation of new protein phosphatase inhibitors from two cyanobacteria species, Planktothrix spp. Journal of Natural Products, 64(8): 1052–1055. DOI: 10.1021/np0005356

Seneviratne SI, Nicholls N, Easterling D, Goodess CM, Kanae S, Kossin J, et al. 2012. Changes in climate extremes and their impacts on the natural physical environment. *In* Managing the risks of extreme events and disasters to advance climate change adaptation. *Edited by* CB Field, V Barros, TF Stocker, D Qin, DJ Dokken, KL Ebi, et al. Cambridge University Press, Cambridge, UK and New York, New York. pp. 109–230.

Smutná M, Babica P, Jarque S, Hilscherová K, Maršálek B, and Haeba M, et al. 2014. Acute, chronic and reproductive toxicity of complex cyanobacterial blooms in Daphnia magna and the role of microcystins. Toxicon, 79: 11–18. DOI: 10.1016/j.toxicon.2013.12.009

Soulis ED, Sarhadi A, Tinel M, and Suthar M. 2016. Extreme precipitation time trends in Ontario, 1960–2010. Hydrological Processes, 30(22): 4090–4100. DOI: 10.1002/hyp.10969

Spoof L, Błaszczyk A, Meriluoto J, Cegłowska M, and Mazur-Marzec H. 2016. Structures and activity of new anabaenopeptins produced by Baltic Sea cyanobacteria. Marine Drugs, 14(1): 8. DOI: 10.3390/md14010008

Sukenik A, Quesada A, and Salmaso N. 2015. Global expansion of toxic and non-toxic cyanobacteria: effect on ecosystem functioning. Biodiversity and Conservation, 24(4): 889–908. DOI: 10.1007/s10531-015-0905-9

Teneva I, Dzhambazov B, Koleva L, Mladenov R, and Schirmer K. 2005. Toxic potential of five freshwater Phormidium species (Cyanoprokaryota). Toxicon, 45(6): 711–725. DOI: 10.1016/j.toxicon.2005.01.018

Thornton J, Steel A, and Rast W. 1996. Reservoirs. *In* Water quality assessments—a guide to use of biota, sediments and water in environmental monitoring. 2nd ed., Vol. 5. *Edited by* D Chapman. E & FN Spon, London, UK.

Vezie C, Brient L, Sivonen K, Bertru G, Lefeuvre JC, and Salkinoja-Salonen M. 1998. Variation of microcystin content of cyanobacterial blooms and isolated strains in Lake Grand-Lieu (France). Microbial Ecology, 35(2): 126–135. PMID: 9541549 DOI: 10.1007/s002489900067

Vollenweider RA. 1968. Scientific fundamentals of the eutrophication of lakes and flowing waters, with particular reference to nitrogen and phosphorus as factors in eutrophication. Technical Report DAS/CS1/68.27. Vol. 3. Organisation for Economic Co-Operation and Development, Paris, France. DOI: 10.1007/BF01597638

Welker M, and Von Döhren H. 2006. Cyanobacterial peptides – Nature's own combinatorial biosynthesis. FEMS Microbiology Reviews, 30(4): 530–563. DOI: 10.1111/j.1574-6976.2006.00022.x

Winslow L, Read J, Woolway R, Brentrup J, Leach T, Zwart J, et al. 2019. rLakeAnalyzer: lake physics tools [online]: Available from cran.r-project.org/package=rLakeAnalyzer.

Winter JG, DeSellas AM, Fletcher R, Heintsch L, Morley A, Nakamoto L, et al. 2011. Algal blooms in Ontario, Canada: increases in reports since 1994. Lake and Reservoir Management, 27(2): 107–114. DOI: 10.1080/07438141.2011.557765

Wood SA, Borges H, Puddick J, Biessy L, Atalah J, Hawes I, et al. 2017. Contrasting cyanobacterial communities and microcystin concentrations in summers with extreme weather events: insights into potential effects of climate change. Hydrobiologia, 785(1): 71–89. DOI: 10.1007/s10750-016-2904-6

Wuebbles D, Meehl G, Hayhoe K, Karl TR, Kunkel K, Santer B, et al. 2014. CMIP5 climate model analyses: climate extremes in the United States. Bulletin of the American Meteorological Society, 95(4): 571–583. DOI: 10.1175/BAMS-D-12-00172.1

Yakobowski SJ. 2008. Ecological factors controlling microcystin concentrations in the Bay of Quinte, Maumee Bay, and three Grand River reservoirs. Master's thesis, University of Waterloo, Waterloo, Ontario. [online]: Available from hdl.handle.net/10012/3548.